Dibenzo-*p*-dioxin. An ab Initio CASSCF/CASPT2 Study of the $\pi-\pi^*$ and n$-\pi^*$ Valence Excited States

Ivan Ljubić* and Aleksandar Sabljić†

Department of Physical Chemistry, Ruđer Bošković Institute, P.O. Box 180, HR-10002, Zagreb, Republic of Croatia

Received: April 11, 2005; In Final Form: July 8, 2005

The $\pi-\pi^*$ and n$-\pi^*$ valence excited states of dibenzo-*p*-dioxin (DD) were studied via the complete active space SCF and multiconfigurational second-order perturbation theory employing the cc-pVDZ basis set and the full π-electron active spaces of 16 electrons in 14 active orbitals. The geometry and harmonic vibrational wavenumbers of the ground state correlate well with the experimental and other theoretical data. In particular, significant improvements over previously reported theoretical results are observed for the excitation energies. All of the $\pi-\pi^*$ excited states exhibit planar D_{2h} minima. Thus no evidence was found for a C_{2v} butterfly-like relaxation, although the wavenumbers of the b_{3u} butterfly flapping mode proved exceedingly low in both the ground $S_0(^1A_g)$ and the lowest dipole allowed excited $S_1(^1B_{2u})$ state. The calculations of oscillator strengths established the $2^1B_{2u} \leftarrow 1^1A_g$ and $2^1B_{1u} \leftarrow 1^1A_g$ transitions as by far the most intense, whereas the only allowed of the n$-\pi^*$ transitions ($^1B_{3u}$) should possess only a modest intensity. Studies into dependence of the oscillator strengths on the extent of the butterfly-like folding showed that the electronic spectrum is more consistent with a folded equilibrium geometry assumed by DD in solution.

Introduction

The polychlorinated derivatives of dibenzo-*p*-dioxin (PCDDs), besides their high acute toxicity, proved very hazardous also in longer terms, because numerous studies established them as tumor promoters and teratogens.[1] Naturally occurring[2] and generated as unwanted byproducts of many industrial processes, mainly iron ore sinter plants and nonferrous metal industry facilities,[3] as well as during incineration of industrial, municipal, and hospital wastes,[4] PCDDs are nowadays recognized as a widely encountered class of pollutants.[5] Despite a considerable decrease in the PCDDs release to the environment throughout the past decade, semivolatility and high resistance to degradation made possible their transport over long distances, with many years old emissions still contributing to current exposure.[5] A major environmental and health concern stems from their solubility in lipids and the consequent tendency toward accumulation in fatty, skin, and liver tissues, whereas the elimination from human body comes about only slowly.[6] A design of efficient methods of detection and photodeactivation of PCDDs calls for further extensive research into their fundamental physical properties.[7] Theoretical studies into the electronic structure of PCDDs, in particular their IR and electronic spectra, have a very important role here.

Dibenzo-*p*-dioxin (DD) stirred a considerable number of experimental and theoretical studies as a nucleus compound and a natural starting point for investigation into PCDDs. The most recent efforts include sub-Doppler high-resolution excitation spectroscopy by Baba et al.,[8] as well as thorough analyses of the condensed phase IR, Raman, and phosphorence spectra on the part of Gastilovich et al.[9] The structure of DD is depicted in Figure 1.

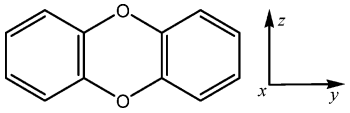

Figure 1. Dibenzo-*p*-dioxin and labeling of the coordinate axes within the D_{2h} point group symmetry.

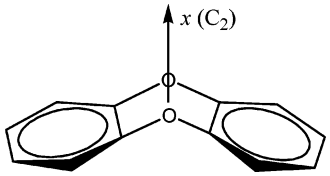

Figure 2. Dibenzo-*p*-dioxin in the C_{2v} butterfly conformation.

In labeling the coordinate axes in the D_{2h} DD molecule, we adopted the recommendation by the IUPAC Commission on Molecular Structure and Spectroscopy,[10] with the *z*-axis passing through the largest possible number of atoms and the *x*-axis perpendicular to the molecular plane (Figure 1). This convention differs from that adopted in the most recent spectroscopical investigation by Baba et al.[8] The correspondence between the molecule fixed axes and the irreducible representations (irreps) of the DD molecular orbitals within the two labeling conventions is the following:

this work	*x*	*y*	*z*	a_g	b_{1g}	b_{2g}	b_{3g}	a_u	b_{1u}	b_{2u}	b_{3u}
ref 8	*y*	*z*	*x*	a_g	b_{3g}	b_{1g}	b_{2g}	a_u	b_{3u}	b_{1u}	b_{2u}

In the so-called butterfly conformation, claimed by some authors to be the equilibrium structure of the ground and/or the lowest excited state (vide infra), the molecule assumes a nonplanar C_{2v} structure, as the one depicted in Figure 2. The butterfly-like bending in DD preserves the σ_{xy} and σ_{xz} reflection planes, whereas only the *x*-axis remains 2-fold (C_2). The middle dioxin ring may thus be twisted to a more favorable boat conformation,

* To whom the correspondence should be addressed. E-mail: iljubic@irb.hr.
† E-mail: sabljic@irb.hr.

10.1021/jp051867s CCC: $30.25
Published on Web 08/20/2005

however, at the expense of less pronounced stabilization via the π-electron delocalization. The angle closed by the two benzene rings commonly serves as a convenient measure of the degree of molecular distortion. From the character tables of the D_{2h} and C_{2v} point groups, on employing the molecule fixed coordinate system (Figure 1) the irreps of the C_{2v} subgroup are correlated with the D_{2h} irreps (in parentheses) as follows: A_1 ($A_g + B_{3u}$), A_2 ($B_{3g} + A_u$), B_1 ($B_{1u} + B_{2g}$), and B_2 ($B_{2u} + B_{1g}$).

The equilibrium structure of DD in the ground state (S_0) has long raised controversies, as to whether the nuclear configuration has a D_{2h} planar form or is bent from the plane as in a butterfly form. The issue is not only of an academic interest, for the reason that certain studies correlate higher ecotoxic properties of some dioxin isomers with their planarity.[11] Thus Colonna et al.[12] measured the nonzero (0.55 D) dipole moment of DD in the benzene solution and showed it to be consistent with a folded conformation, in which the two benzene rings close the angle of 164°. An analogous conclusion was reached on the grounds of dipole polarization studies, albeit with a somewhat larger dipole moment (0.64 D) determined.[13] A semiempirical extended Hückel theory (EHT) for an isolated molecule yielded the planar minimum, although the conformational energy was found to be rather insensitive to changes in the angle between the two benzene rings.[12] It was concluded that the DD structure must be markedly nonrigid in solution, owing to a very low barrier to the butterfly flapping motion. The analogous structural peculiarities, planar ground state minima coupled with very low barriers to the butterfly-like folding, were observed at the B3LYP/6-31G(d) level for the most toxic of dioxin congeners, tetrachlorinated DDs.[14] The electronic transitions and oscillator strengths calculated at the semiempirical SCF-PPP-CIS level[12,15] were in a fair agreement with the absorption spectrum of DD in heptane solution due to Lamotte and Berthier.[16]

Zimmermann et al.[17] determined the first ionization energy of DD (7.598 ± 0.002 eV) using the resonance-enhanced two-color two-photon ionization technique. These authors also recorded a clearly structured intermediate state spectrum of the first excited singlet state S_1. Apart from the most intense vibronic line at $\tilde{\nu}(0-0) + 22$ cm^{-1}, attributed to the out-of-plane butterfly flapping mode of the S_1 state, the spectrum exhibited an unusual number of low-frequency modes (<200 cm^{-1}). On account of the similarity of the DD vibronic spectrum to that of the first excited state of 9,10-dihydroanthracene, it was inferred that the most stable conformation of DD in the S_1 state should be different from the S_0 state. Finally, on the basis of the semiempirical AM1 and ab initio calculations, it was concluded that a folded minimum is to be expected in the ground state and a planar one in the S_1 excited state.[17] However, recent high-resolution spectroscopic studies of DD[8,9] eventually seem to settle the controversies, at least for the crystalline and gas phase, in favor of the planar (D_{2h} point group symmetry) ground state equilibrium structure of DD.

In studies of the lowest allowed $S_1 \leftarrow S_0$ transition using the technique of sub-Doppler high-resolution excitation spectroscopy,[8] two bands were located at 33773 and 33795 cm^{-1} (4.19 eV), and the corresponding states designated as $S_1(\upsilon' = 0)$ and $S_1(\upsilon' = 0 + 22$ cm$^{-1})$, respectively. The determined molecular constants for the ground $S_0(\upsilon'' = 0)$, as well as the excited S_1-$(\upsilon' = 0)$ and $S_1(\upsilon' = 0 + 22$ cm$^{-1})$, state subsequently enabled the latter to be identified as $S_1(\upsilon' = 1)$ of the a_g component of the butterfly flapping mode. The transition moment parallel to the longer axis (y) in the molecular plane identified the corresponding transition as $^1B_{2u}$ within the present labeling convention ($^1B_{1u}$ in the original work).[8]

The equilibrium structure of the S_1 excited state appears for now to provide yet another controversy. Namely, on grounds of the selection rules and the vibronic structure in the condensed phase IR and Raman spectra, Gastilovich et al.[9c] concluded that the S_1 state should be planar with the D_{2h} symmetry retained. In contrast, on grounds of nonzero inertial defect observed in the S_1 state, Baba et al.[8] argued that a C_{2v} butterfly minimum is assumed, with the benzene rings closing the equilibrium angle of 170.6° and 173.4° in the S_1 ($\upsilon' = 0$) and the $S_1(\upsilon' = 0 + 22$ cm^{-1}) states, respectively. The latter authors also performed RCIS calculations and obtained the excitation energies and oscillator strengths for several lower singlet states of DD utilizing the B3LYP/6-311G(d,p) optimized geometries. The results proved disappointing, however, as the excitation energy for the lowest allowed transition was placed 14 000 cm^{-1} ($\sim$1.7 eV) too high. Furthermore, contrary to the experimental evidence on the nonplanarity of the S_1 state, the B3LYP/6-311G(d,p) method resulted in the planar D_{2h} S_1 minimum.[8]

The lowest singlet−triplet (T_1) transition was observed in a fine structured phosphorescence spectrum of DD in an *n*-hexane matrix at 4.2 K.[9a,c] To decide on the nuclear configurations of the S_0, S_1, and T_1 states, the Herzberg−Teller selection rules were used for the case of D_{2h} and C_{2v} point group symmetries. Thus the planarity of the T_1 state was inferred on grounds of the absence of overtones for the fundamental a_u and b_{3u} modes.[9c] The two 0−0 Shpol'skii lines, originating from the phosphorescence from two different sites in the matrix, were located at 25 595 and 25 562 cm^{-1} ($\sim$3.17 eV). On account of their exceedingly weak intensities, as for orbitally forbidden transitions, the T_1 state was assigned as $^3B_{3g}$.

The aim of the present study is to explore a number of singlet and triplet $\pi-\pi^*$ and $n-\pi^*$ valence excited states of DD. To accomplish this, we opted for the multiconfigurational complete active space SCF method (CASSCF)[18] in obtaining the optimized geometries and zeroth-order wave functions, followed by the multireference perturbational approach to the second order (CASPT2)[18b,19] in accounting for the dynamical electron correlation. The remarkable performance of the CASSCF/CASPT2 approach in studying reactions[20] and potential energy surfaces of molecular ground and excited states, including assignment of vibrational[21] and electronic[22] spectra, is by now well documented in numerous studies, which encompassed a wide variety of molecules.[23] The previous theoretical studies on the structure, reactions, and the IR and electronic spectra of DD and its derivatives relied on the Hartree−Fock (HF), density functional theory (DFT), and semiempirical approaches.[14,24] Reliable high-level ab initio studies are currently lacking, however, so that the present study also aims at a certain effort in this respect.

Computational Methods

The CASSCF method was utilized in geometry optimizations and subsequent harmonic frequency calculations. This method essentially corresponds to a full configuration interaction, including simultaneous orbital optimization, performed in the subspace of active orbitals, which are selected on the grounds of chemical intuition as the most important ones for the problem in question.[18b] Thus, in studying the $\pi-\pi^*$ transitions the entire π-orbital space was chosen as active, whereas in studying the $n-\pi^*$ transitions the orbitals pertaining to the p_x lone pairs on the two oxygen atoms were excluded from the active space and

replaced with the in-plane p_z lone pairs. These choices resulted in large active spaces of 16 electrons distributed among the 14 active orbitals in all space and spin symmetry allowed ways. The ground and excited state structures were obtained as the energy minima upon restricting the CASSCF wave functions to a desired space symmetry (vide infra).

The geometry optimizations were at first carried out by making use of the full D_{2h} point group symmetry. Subsequently, the stability of the optimized structures was verified by reducing the symmetry to the C_{2v} subgroup, thus allowing for a possibility of an out-of-plane butterfly-like relaxation. In calculating the $\pi-\pi^*$ transitions, the space of 14 p-orbitals perpendicular to the molecular plane was used. Within the $D_{2h}(C_{2v})$ point groups, this space is reduced to $3b_{1g}(b_2)$, $4b_{2g}(b_1)$, $4b_{3u}(a_1)$, and $3a_u(a_2)$ MOs, using the molecule fixed coordinate frame as in Figure 1. In calculating the $n-\pi^*$ transitions, the b_{3u} and b_{2g} orbitals corresponding to the two oxygen lone pairs were replaced with the in-plane lone pairs of a_g and b_{1u} symmetry. By doing this, however, it was no longer possible to allow for a C_{2v} relaxation, because one cannot distinguish between the oxygen lone pairs using the symmetry arguments, because of the fact that the DD molecular plane formally vanishes. Thus, unlike the $\pi-\pi^*$, all of the $n-\pi^*$ transitions had to be studied within the D_{2h} point symmetry to enforce the desired active space. The symmetry species of excited states are determined by the direct products of irreps of the orbitals involved in the transition. Thus, of the $\pi-\pi^*$ transitions one expects the A_g, B_{3g}, B_{1u}, and B_{2u} states, and of the $n-\pi^*$ transitions the A_u, B_{1g}, B_{2g}, and B_{3u} states. Of these, provided the planar DD conformation is retained, the only dipole allowed transitions will be to the three B ungerade states. Also interesting are the transitions to the $2A_g$, $1B_{2g}$, and $1B_{1g}$ states, which either may gain intensity via the vibronic coupling with the b_{3u} butterfly folding mode or become orbitally allowed upon the butterfly-like relaxation to the C_{2v} point symmetry, thus matching the $2A_1 \leftarrow 1A_1$, $B_1 \leftarrow A_1$, and $B_2 \leftarrow A_1$ transitions, respectively.

At the CASSCF optimized geometries the dynamic electron correlation was accounted for via the CASPT2 method by taking the CASSCF wave functions as the zeroth-order references. The CASPT2 method is formulated as a perturbation expansion up to the second order with excitations from the CASSCF reference.[19] A modification of the zeroth-order Hamiltonian, designated g_2, was applied throughout, to mitigate a systematic error of overestimation of the stability of open shells in CASPT2.[25] The weights of the CASSCF(16,14) references were in a narrow range 0.61−0.64, which made possible a sensible comparison between the corresponding CASPT2 energies. In particular, the ground state weight of the CASSCF reference equals 0.635, without a single larger contribution to the CASPT2 energy listed. This convinced us that around 60% reference weight is physically plausible within the used computational approach.

The active occupancies (please refer to Supporting Information) were indicative of a pronounced multiconfigurational nature of the DD molecule, including also its ground state equilibrium structure. Numerical experiments demonstrated that orbitals with active occupancies in the range 0.020−1.980 are important for description of near-degeneracy effects, whereas those with the occupancies close to 2.0 or 0.0 should be excluded from the active space to provide sensible zeroth-order references.[26] Nevertheless, the $1b_{3u}$ and $1b_{2g}$ orbitals, occupying principally the region of p_x lone pairs on the two oxygen atoms were kept in the active space, although their active occupancies are very close to 2.0 for the majority of the $\pi-\pi^*$ states studied. In connection to this, a well-established approach is to enlarge the active space with additional virtual orbitals correlating the lone pairs as well.[22] In the particular case of DD, however, providing further active orbitals would have enlarged the active space prohibitively. Although the lone pairs thus remained considerably less correlated to the rest of the molecular π-system, it transpired imprudent to leave them out altogether (thus creating a CASSCF(12,12) reference), because of severe intruder problems. These are, if affordable, preferably solved by including all those inactive orbitals that bring about large contributions to the CASPT2 energy, rather than having recourse to the level shift (CASPT2-LS) technique.[18b,27] Thus, we decided to stick to the full π-orbital active space in all the calculations on the $\pi-\pi^*$ states, but were forced to intruduce the CASPT2-LS in passing to the $n-\pi^*$ states, where excluding $1b_{3u}$ and $1b_{2g}$ was mandatory to keep the size of the active space manageable. In CASPT2-LS the spectrum of the zeroth order Hamiltonian is suitably shifted to eliminate the effects of the intruder states. The final second-order energy is the back-corrected one, whereby the dependences upon the level shift parameter are removed to the first order.[18b,27] We also tested an imaginary level shift technique as formulated by Forsberg and Malmqvist.[28] The imaginary shift, unlike the real, does not deal with the intruders by merely shifting them, which can cause new singularities, but rather moving them away from the real axis.

The standard Dunning's correlation consistent cc-pVDZ basis set[29] contracted to (3s2p1d) on the C and O atoms and (2s1p) on the H atom was used, which totaled 236 basis functions in DD. As this basis set was not designed to describe the core correlation, all CASPT2 calculations were performed with the inner 1s shells on the O and C atoms frozen. Presently no larger or more flexible basis sets proves affordable in calculations on this scale. Likewise, more detailed studies into possibilities of valence−Rydberg mixings would involve extensions of basis sets with diffuse (Rydberg-type) functions, as well as testing larger active spaces,[22] neither of which is feasible at present. It has been observed, however, that use of large and self-contained active spaces, as is the full π-space used here, generally aids in avoiding contamination of the CASPT2 results due to interaction with the near-lying Rydberg states.[30]

All the electronic structure calculations were performed with *MOLCAS* Version 6.0 program package.[31] The CASSCF transition dipole moments (TDMs) in length representation were calculated by employing the RASSI module available in *MOLCAS*.[32] The oscillator strengths f were calculated from the CASSCF TDMs and the CASPT2 vertical excitation energies ΔE (in hartrees) according to

$$f = \frac{2}{3}(\mathrm{TDM})^2 \Delta E \qquad (1)$$

Results and Discussion

A pictorial representation (using *MOLDEN*[33]) of the (16,14) active space of DD, as well as the corresponding active occupancies of the ground and the excited states, are available as Supporting Information. From the active occupancies, the trends in density transfer upon transitions do not support the view that the lowest states of DD are characterized by the transfer of charge from the oxygen atoms to the π-system of the benzene rings.[9b] Rather the p_x oxygen lone pairs have only a minor role, and a redistribution of density to the antibonding orbitals within the rings, whereby the C−C bonds are generally weakened, is what primarily takes place.

TABLE 1: Geometric Parameters (D_{2h} Symmetry; Bond Distances in Angstroms; Angles in Degrees) of the Ground (^1A_g) and Excited ($\pi-\pi^*$ and n-π^*) Singlet and Triplet States of Dibenzo-*p*-dioxin at the CASSCF(16,14)/cc-pVDZ Level

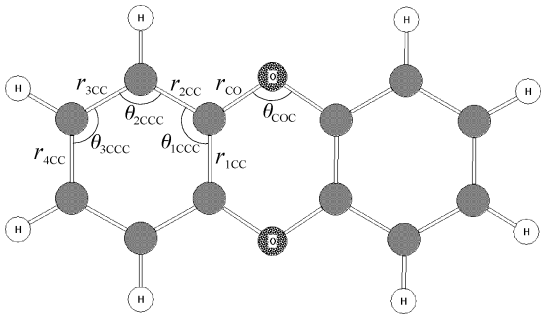

	r_{CO}	r_{1CC}	r_{2CC}	r_{3CC}	r_{4CC}	θ_{COC}	θ_{1CCC}	θ_{2CCC}	θ_{3CCC}
					$\pi-\pi^*$				
1^1A_g	1.363	1.395	1.392	1.397	1.397	116.8	120.1	119.9	120.0
exp[a]	1.384		1.366−1.384; $r_{mean}=1.377$			116.5	119.2−120.8; $\theta_{mean}=120.0$		
1^1B_{3g}	1.327	1.431	1.413	1.374	1.445	119.8	119.8	119.9	120.4
1^1B_{2u}	1.353	1.411	1.412	1.414	1.414	118.1	120.6	118.9	120.5
1^1B_{1u}	1.339	1.436	1.403	1.406	1.465	120.2	120.4	119.9	119.7
1^3A_g	1.350	1.413	1.408	1.410	1.407	117.8	120.8	118.4	120.9
1^3B_{3g}	1.346	1.440	1.401	1.390	1.446	119.2	120.0	119.9	120.1
1^3B_{2u}	1.350	1.417	1.407	1.413	1.405	119.0	120.7	118.5	120.8
1^3B_{1u}	1.365	1.385	1.420	1.426	1.391	115.5	120.5	119.3	120.2
					n−π^*				
1^1A_g	1.365	1.394	1.391	1.397	1.397	116.7	120.2	119.9	120.0
1^1A_u	1.338	1.469	1.397	1.385	1.424	125.9	118.6	121.5	119.9
1^1B_{1g}	1.345	1.430	1.401	1.423	1.377	126.9	120.4	118.4	121.1
1^1B_{3u}	1.354	1.420	1.404	1.415	1.382	123.1	120.4	118.6	121.0
1^1B_{2g}	1.362	1.470	1.379	1.403	1.424	125.1	118.8	121.9	119.3
1^3A_u	1.337	1.470	1.399	1.384	1.423	125.9	118.5	121.5	120.0
1^3B_{1g}	1.344	1.430	1.401	1.423	1.377	126.9	120.4	118.5	121.1
1^3B_{3u}	1.351	1.423	1.402	1.417	1.381	123.4	120.3	118.7	121.0
1^3B_{2g}	1.362	1.473	1.380	1.402	1.422	125.0	118.7	121.9	119.4

[a] The X-ray diffraction geometric parameters of the ground state from ref 34.

A. Geometrical Parameters and Harmonic Wavenumbers. Geometrical parameters of the ground and excited states of DD optimized upon constraining the wave function to a desired space-spin symmetry are listed in Table 1.

The ground, as well as all the singlet and triplet $\pi-\pi^*$ excited states exhibit D_{2h} symmetry at the CASSCF/cc-pVDZ level, employing the full π-orbital active spaces. In other words, all of the optimizations carried out in the C_{2v} symmetry, in the sense of allowing for the butterfly-like relaxation, resulted in the CASSCF structures and CASSCF(CASPT2) energies that were identical to those of the D_{2h} optimized minima. Overall, at the used theoretical level no tendency was found for symmetry breaking in the ground or excited states of the DD molecule. Such a conclusion, with regard to the planar DD structures in case of the S_0 (^1A_g), $S_1(1^1B_{2u})$, and $T_1(1^3B_{3g})$ states, agrees with that reached by Gastilovich et al.,[9] whereas in case of the S_1 state it opposes the experimental evidence gathered by Baba et al.[8] However, the potential for the butterfly motion in both, S_0 and S_1, states is remarkably flat, as is revealed by the harmonic wavenumbers analysis (vide infra), as well as calulations on the folded DD geometries (section B).

The CASSCF(16,14)/cc-pVDZ ground state (1^1A_g) geometrical parameters of DD, with the exception of angles, do not exhibit a particularly good agreement with the parameters derived from the X-ray diffraction data.[34] Apart from the expected discrepancies between the gas and crystalline phase, it should be noted that the reported structure[34] itself shows certain inconsistencies (on order of 0.01 Å) in lengths of chemically equivalent bonds, as well as alterations in C−C bonds in a range that is not predicted by any of the employed theoretical methods. For this reason, only the average values of the corresponding experimental parameters are given in ref 34 and are as such quoted in Table 1. Overall, the computed geometrical parameters should be more credible than those derived from the X-ray results. This finds further support in the calculated rotational constants ($A = 0.072$ cm^{-1}, $B = 0.016$ cm^{-1}, and $C = 0.013$ cm^{-1}), which are in excellent agreement with the most recent experimental data.[8] A comparison with other theoretical approaches shows that, of explicitly correlated bonds, the C−O bond length remains very close to the HF/6-311G(d,p)[24d] value of 1.361 Å, whereas the C−C bonds are similar to the ones from the B3LYP/6-311G(d,p) level (in the 1.388−1.397 Å range),[24b] albeit with differences in ordering of the C−C bond lengths.

Geometrical parameters for the $1B_{2u}$ state (S_1) are not in good agreement with the parameters calculated at the CIS/6-31G-(d,p) level.[24c] In particular, the CIS C−C bond lengths range from 1.366 to 1.435 Å, whereas at the CASSCF(16,14)/cc-pVDZ level they differ negligibly. A further indication of a poor performance of the CIS method in the case of DD is provided by the CIS excitation energies[8] (Table 3), which considerably exceed the experimental and other theoretical results.

Table 2 lists the CASSCF(16,14)/cc-pVDZ calculated, as well as the experimental vibrational wavenumbers, for the ground state DD derived from the solid state IR, Raman, and phosphorescence spectra.[9] The correlation coefficient between the two sets equals 0.9974. All the CASSCF wavenumbers are scaled by 0.9379, which minimizes the sum of squared differences between the calculated and experimental wavenumbers for the ground state. Upon scaling, the mean absolute error

TABLE 2: Harmonic CASSCF(16,14)/cc-pVDZ (calc) and Experimental[9] (exp) Vibrational Wavenumbers (cm^{-1}) of the Ground (^1A_g) and the First Allowed Excited State ($^1B_{2u}$) of Dibenzo-*p*-dioxin[a]

a_g		b_{3u}		b_{2u}		b_{1g}		b_{3g}		a_u		b_{1u}		b_{2g}	
calc	exp	calc	exp	calc	exp	calc	exp	calc	exp	calc	exp	calc	exp	calc	exp
							^1A_g (S_0)								
393	397	20	70[b]	615	610	259	240	443	450	127	155	238	245	231	278
575	564	295	308	836	830	438	450[c]	536	534	522	543	676	676[b]	530	533[b]
733	726	449	448	1029	1030	725	762	912	898	652	706	873	850	668	748
1025	1030	725	748	1116	1150	892	943[b]	1100	1094	812	843	1121	1118	814	898[c]
1128	1154	892	922	1217	1295			1215	1192	926	–	1235	1200	927	977[b]
1228	1226			1352	1400			1309	1317[b]			1307	1308		
1261	1324			1548	1495			1483	1452[b]			1495	1465		
1543	1500			1619	1590			1627	1586			1669	1627		
1652	1621			3151				3137				3137			
3151				3167				3162				3162			
3167															
							$^1B_{2u}$ (S_1)								
386		59	22	583		211		437		114		224		226	
540		268		918		375		513		435		650		460	
709		386		1158		625		903		545		864		569	
977		629		1186		746		1059		670		1084		675	
1160		747		1472				1203		814		1238		815	
1241				1535				1314				1284			
1483				1589				1446				1446			
1528				2184				1596				1626			
1634				3159				3145				3144			
3159				3311				3174				3175			
3179															

[a] The CASSCF wavenumbers are scaled by the factor of 0.9379. [b] Calculated using the GF matrix semiempirical approach.[9] [c] Ambiguous assignment; not clear whether the mode is in-plane or out-of-plane.[9]

TABLE 3: Excitation Energies in eV (Vertical T_v and Adiabatic T_e (T_0 if ZPE Corrected)) of Dibenzo-*p*-dioxin at the CASPT2(16,14)/cc-pVDZ Level with the g_2 Modification of the Zeroth-Order Hamiltonian[a]

$\pi-\pi^*$	T_v	T_e (T_0)	exp	log ϵ	e	f	n-π^*	T_v
1^1B_{3g}	4.04	3.91			5.62	4.00	^1A_u	6.50
1^1B_{2u}	4.28	4.12 (4.10)	4.1874,[b] 4.13[d]	shoulder[d]	5.90	4.13	$^1B_{1g}$	6.99
1^1B_{1u}	5.81	5.74	5.44[d]	4.73[d]	6.43	4.58	$^1B_{3u}$	7.15
2^1A_g	4.42		4.29[d]	3.87[d]	5.92		$^1B_{2g}$	7.99
2^1B_{3g}	7.14				7.45		^3A_u	6.42
2^1B_{2u}	5.60		5.58[d]	4.64[d]	7.53	5.64	$^3B_{1g}$	6.88
2^1B_{1u}	6.08		6.11[d]	weak[d]		6.11	$^3B_{3u}$	7.00
1^3A_g	3.91	3.77				4.30	$^3B_{2g}$	7.85
1^3B_{3g}	3.43	3.12	3.1693[c]			3.52		
1^3B_{2u}	4.01	3.85				4.29		
1^3B_{1u}	3.98	3.85				3.62		
2^3A_g	5.32							
2^3B_{3g}	4.17							
2^3B_{2u}	5.07							
2^3B_{1u}	4.48							

[a] The values for the π^* transitions are obtained with the recommended value of the imaginary shift ($\sigma = 0.20$ hartree; section C). [b] Reference 8. 1^1B_{2u} state via sub-Doppler high-resolution excitation spectroscopy. [c] Reference 9c. 1^3B_{3g} state via Shpol'skii phosphorence in *n*-hexane matrix. [d] Reference 16. Molar absorption coefficients (ϵ) and peaks from the spectrum in heptane solution. [e] RCIS method on B3LYP/6-311G(d,p) optimized geometries (ref 8). [f] INDO/S-CI semiempirical method + shift to lower frequencies by 7000 cm^{-1} (ref 9b).

in calculated wavenumbers is reduced to 26.5 cm^{-1}, with the two largest errors of 80 and 84 cm^{-1} occurring in a relatively small set of b_{2g} (out-of-plane) modes derived from the Raman spectrum.[9b] Overall, the calculated values correlate very well with the experimental data, with the average relative error of 4.7%. This reduces to only 3.4%, if by far the largest relative error in the butterfly flapping mode (71%) is discarded. The value of 70 cm^{-1} for this mode appears exaggerated, knowing it was not determined directly from the spectrum, but by the GF matrix semiempirical approach assuming the X-ray geometric parameters of DD.[9a] This view is further supported by the CASSCF value of only ~20 cm^{-1}, which is quite similar to the values for the butterfly mode in tetrachlorinated DD derivatives obtained via the scaled quantum mechanical (SQM) B3LYP/6-31G(d) method.[14]

Of the wavenumbers for the first allowed ($^1B_{2u}$) excited state, the single unambiguously assigned and accurately measured value[8,9,17] of 22 cm^{-1} for the butterfly flapping mode does not agree well with the calculated value of ~60 cm^{-1}. The calculated larger value for this mode as compared to the ground state is due to the peculiarities of the electron density transfer upon the $1^1B_{2u} \leftarrow 1^1A_g$ transition, which tend to strengthen the C−O bond and weaken the C−C bonds. Similar trends in changes of the bond lengths are in fact observable for the majority of the $\pi-\pi^*$ states, with the sole exception of 1^3B_{1u}. As a result, the barrier for twisting the middle ring toward a boat conformation becomes somewhat higher. In the 1^1B_{2u} state, the amount of the electronic density transferred to the $3b_{1g}$, $3b_{2g}$, and $2a_u$ antibonding orbitals (in the range of 0.2−0.4*e*) is only moderate compared to the higher excited states. This is also reflected in a comparatively minor weakening of the C−C bonds (Table 1) and in the wavenumbers of the 1^1B_{2u} state (Table 2), which are in general not particularly reduced compared to the ground state. A host of presently unassigned very low-frequency modes occurring in the intermediate S_1 ionization spectrum[17] (7 of them below 200 cm^{-1}) is thus not confirmed at the used theoretical level, and its origin remains uncertain.

B. $\pi-\pi^*$ Transitions. The calculated and experimental excitation energies for the singlet and triplet $\pi-\pi^*$ and n−π^* transitions are listed in Table 3. The correlation between calculated transitions and the DD spectral peaks in heptane solution[16] is tabulated as proposed in ref 12. Table 4 collects the calculated oscillator strengths (length representation) corresponding to the dipole allowed transitions. The experimental spectrum with the superimposed CASPT2 excitation

TABLE 4: Oscillator Strengths *f* (Length Representation) of the Dipole Allowed Electron Transitions from the ^1A_g Ground State of Dibenzo-*p*-dioxin[a]

	state				
	$1B_{2u}$	$1B_{1u}$	$2B_{2u}$	$2B_{1u}$	$1B_{3u}$
polar. axis	*y*	*z*	*y*	*z*	*x*
$\|TDM\|^2$	0.131	0.208	2.756	0.423	2.89×10^{-4}
f	1.37×10^{-2}	2.96×10^{-2}	3.78×10^{-1}	6.01×10^{-2}	5.24×10^{-5}

[a] The transition dipole moments (TDMs in au) are between the corresponding CASSCF(16,14)/cc-pVDZ wave functions obtained in the ^1A_g equilibrium geometry. The vertical energy differences are used, calculated at the CASPT2(16,14)/cc-pVDZ level with the g_2 modified zeroth-order Hamiltonian.

energies and CASSCF relative intensities, as well as simulated spectra (original and fitted, vide infra), are shown in Figure 3.

The CASPT2 excitation energies for the $\pi-\pi^*$ and $n-\pi^*$ triplet states are in all cases lower than those of the corresponding singlets. For the two most accurately measured and unambiguously assigned transitions, $1^1B_{2u} \leftarrow 1^1A_g$ ($S_1 \leftarrow S_0$) and $1^3B_{3g} \leftarrow 1^1A_g$ ($T_1 \leftarrow S_0$), the CASPT2 energies are seen to be in very good agreement with the experimental values. In particular, the result for the $S_1 \leftarrow S_0$ excitation energy is much improved over the previous studies, which employed semiempirical, DFT, and RCIS methods.[8,9,12] Even though the sets of DZP quality are minimal for a sensible correlated treatment, the calculated excitation energies fall well within the empirically established error bounds ($\pm$0.3 eV) for CASPT2.[22] In fact, detailed studies into the effects of the basis sets size on the excitation energies[30] showed that the results using contractions of the (4s3p1d) quality on the first row atoms and (2s) on hydrogens agreed within 0.1 eV with those obtained using the most extended basis sets. In particular, the addition of the single set of polarization functions (1d) resulted in by far the most important improvement over the minimal basis set.[30] Considering this, the very good performance of the cc-pVDZ set comes as no surprise, and it offers a certain trustworthiness in assigning the remaining, much less explored transitions.

Henceforth, all the discussed transitions are implicit as the spin allowed, so that we omit the spin superscript from the designations of the states. The experimental spectrum (Figure 3) exhibits two distinct features, the high-intensity band system in the 200−235 nm region and the broader low-intensity band system in the 265−310 nm region ending with the shoulder. Our calculations show that the former region comprises the three most intense dipole allowed transitions (to the $1B_{1u}$, $2B_{1u}$, and $2B_{2u}$ states), whereas the $1B_{2u} \leftarrow 1A_g$ transition and the vibronic allowed (or dipole allowed in the C_{2v} symmetry) $2A_g \leftarrow 1A_g$ may account for the latter region. As regards the suggested correlation[12] between the calculated and experimental peaks (Table 3), by far the largest discrepancy is found for the alleged $1B_{1u} \leftarrow 1A_g$ transition, where apart from the 0.30 eV higher CASPT2 excitation energy, the modest CASSCF oscillator strength fails in reproducing the highest measured log ϵ value of 4.73. Instead, the high-intensity band system in the 200−235 nm region can be observed as dominated by the $2B_{2u} \leftarrow 1A_g$ and $2B_{1u} \leftarrow 1A_g$ transitions, which is further confirmed by analyzing the trends in oscillator strengths in the course of the butterfly-like folding of DD (Table 5). The CASPT2 vertical excitation energies indicate that the $1B_{1u}$ and $2B_{1u}$ states are rather near-lying (Table 3), whereas the CASSCF oscillator strengths calculated in the D_{2h} and C_{2v} symmetries assign the second strongest intensity to the $2B_{2u} \leftarrow 1A_g$ transition (Tables 4 and 5) and only a weak one to the $1B_{1u} \leftarrow 1A_g$. Thus the calculated intensities of these two bands are effectively interchanged as compared to the experimental assignments[16] (Table 3). Nonetheless, a small red shifting of the $2B_{1u}$ state (within the normal error bars for the CASPT2 excitation energies[22]) can make for an excellently reproduced shape of this region of the spectrum in solution (vide infra).

Table 5 collects the changes in the squared transition dipole moments for the dipole allowed transitions in the event of the butterfly-like motion, calculated for the three bent structures, *a*, *b*, and *c*. These structures emerged as intermediate in the course of optimization of the ground state DD, which was constrained to the C_{2v} symmetry and initiated from a very folded geometry ($\alpha \sim 120°$). The structures *a*, *b*, and *c* are taken from the later stages of the optimization, so that the corresponding bonds and angles may be considered sufficiently relaxed and reasonably representative of the trends in geometric parameters during the butterfly motion. The ranges of folding, expressed in the angles α and β, are similar to those derived in rationalizing the measured nonzero dipole moment of DD in nonpolar solvents.[12,13] The course of the optimization indicated a remarkably flat potential, as illustrated by the total CASSCF energy changing by less than 2 kcal mol^{-1} with the change of 30° in α. Thus, even in the absence of a permanent butterfly-like relaxation to the C_{2v} symmetry, the transitions that are vibronic allowed via coupling with the butterfly mode should noticeably affect the appearance of the spectrum.

Of the $\pi-\pi^*$ transitions, only the $2A_1 \leftarrow 1A_1$ ($2A_g \leftarrow 1A_g$) becomes dipole allowed upon the relaxation to the C_{2v} symmetry. The size of an analogous effect expected for the $n-\pi^*$ $B_2 \leftarrow 1A_1$ ($1B_{1g} \leftarrow 1A_g$) and $B_1 \leftarrow 1A_1$ ($1B_{2g} \leftarrow 1A_g$) transitions could not be tested, because the desired active space cannot be imposed within the butterfly C_{2v} symmetry, provided the active space does not become larger than (16,14). The lowest-lying of the $\pi-\pi^*$ and $n-\pi^*$ transitions, $1B_{3g} \leftarrow 1A_g$ and $1A_u \leftarrow 1A_g$ (Table 3), remain forbidden, either upon the butterfly-like relaxation, or likewise via the vibronic coupling with the butterfly mode.

Simulations of the spectrum employing a few standard line shapes[36] indicate that, in the structures folded to a similar extent as in nonpolar solvents,[12,13] the intensity gained by the now dipole allowed $2A_1 \leftarrow 1A_1$ transition is too small to account for the shape of the 265−310 nm region (Figure 3). Instead, in the recent study of the DD spectrum by the INDO/S-CI semiempirical method, followed by shifting the calculated peaks by 7000 cm^{-1} toward lower frequencies[9b] (Table 3), the $^1B_{1u} \leftarrow A_g$ transition was eventually positioned in the proximity of the shoulder ($\sim$270 nm). This, however, stands in a sharp contrast with the present work, as well as the previous theoretical attempts at assigning the experimental spectrum.[8,12,15]

The original theoretical spectral curve (theor. original; Figure 3) was obtained by fitting on the Lorentzian line shapes, using the common half-bandwidth parameter of 1650 cm^{-1} and vertical excitation energies and oscillator strengths as calculated in the slightly folded geometry *c* ($\alpha = 169.1°$; Table 5). The trends in intensities observable upon the gradual folding of DD generally lead to a more faithful reproduction of the experimental spectrum in solution. Thus the difference in intensities between the transitions to the $2B_{1u}$ and $2B_{2u}$ states is reduced, whereby the bands in the 200−235 nm region bear more similarity to the observed pattern. At the same time, the $2A_g \leftarrow 1A_g$ becomes stronger and the $1B_{2u} \leftarrow 1A_g$ weaker, which is necessary to create the observed shoulder. A theoretical curve can be obtained (Figure 3, theor. fitted), which reproduces remarkably well all of the features of the spectrum in solution,

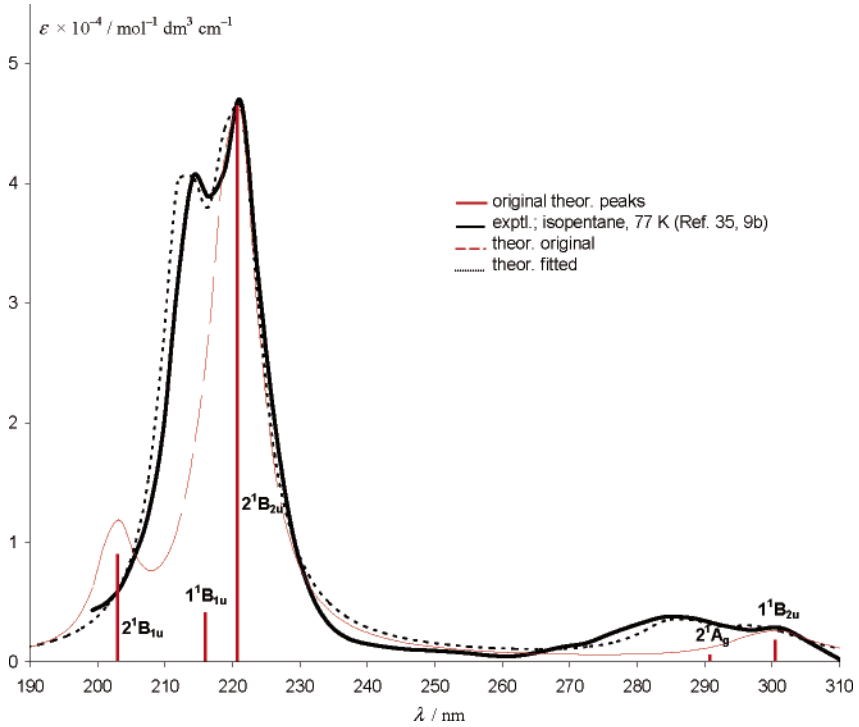

Figure 3. Experimental spectrum of dibenzo-*p*-dioxin in solution, with the two superimposed simulated spectra. The "theor. original" curve uses vertical band centers and oscillator strengths as calculated in the geometry *c* (Table 5). The "theor. fitted" curve employs parameters fitted to faithfully reproduce the appearance of the experimental spectrum (Table 6).

TABLE 5: Dependence of the $\pi-\pi^*$ Transition Dipole Moments Squared (Length Representation) for the Three Butterfly-Folded Geometries at the CASSCF(16,14)/cc-pVDZ Level

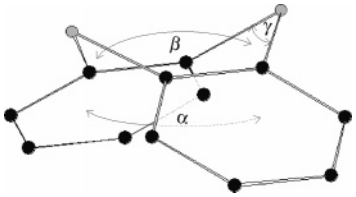

	geometry[a]			
state	*a*	*b*	*c*	*d*
$1B_{2u}$	0.0795	0.1050	0.1325	0.1310
$1B_{1u}$	0.0630	0.1452	0.1706	0.2079
$2B_{2u}$	1.0486	1.5129	1.8660	2.7556
$2B_{1u}$	0.6068	0.4761	0.3881	0.4225
$2A_g$	0.0037	0.0028	0.0017	0.0000

[a] Geometries: (*a*) $\alpha = 161.4°$; $\beta = 160.1°$; $\gamma = 111.2°$; (*b*) $\alpha = 164.9°$; $\beta = 160.6°$; $\gamma = 114.2°$; (*c*) $\alpha = 169.1°$; $\beta = 163.1°$; $\gamma = 116.2°$; (*d*) 1^1A_g minimum, $\alpha = 180.0°$; $\beta = 180.0°$; $\gamma = 116.8°$.

provided certain adjustments in the oscillator strengths and band centers are made, while retaining the Lorentzian line shapes and the common half-bandwidth of 1650 cm^{-1}. The comparison between the adjusted set of parameters and the genuine oscillator strengths and band centers as calculated in the geometry *c* are summarized in Table 6.

From Table 6 we first note that the vertical $2A_g \leftarrow 1A_g$ excitation energy of 291 nm (4.26 eV) evaluated in the folded geometry *c* is much closer to the measured absorption at 4.29 eV[16] than the energy evaluated in the D_{2h} geometry (Table 3). It is further seen that the $2A_g$ and $2B_{1u}$ are the only band centers that need be nonnegligibly shifted, the first one being blue-shifted by 5 nm and the second one red-shifted by 9 nm. In the geometry *c*, the CASSCF oscillator strengths derived from the

TABLE 6: Comparison between the Two Sets of Band Centers (nm) and Oscillator Strengths[a]

		1^1B_{2u}	2^1A_g	2^1B_{2u}	1^1B_{1u}	2^1B_{1u}
band centers	geometry *c*	300	291	221	216	203
	fitted	299	286	221	216	212
f	geometry *c*	0.0134	0.0002	0.2571	0.0241	0.0547
	fitted	0.0110	0.0150	0.2200	0.0265	0.1750

[a] The first set corresponds to the CASSCF/CASPT2 calculations carried out in the folded DD geometry *c* (Table 5; theor. original, Figure 3). The second one is a fitted set, used in obtaining a faithful reproduction of the experimental spectrum (theor. fitted, Figure 3).

CASPT2 vertical energies are in a very good agreement with the fitted parameters for the three states ($1B_{2u}$, $2B_{2u}$, and $1B_{1u}$). On the other hand, in particular for the $2A_g$ state a large adjustment in the oscillator strength has to be made, whereupon it is 75 times increased. Because such a dramatic increase is not exhibited within larger folding amplitudes (Table 5), either the CASSCF result for the oscillator strength is in a significant error here, or another very efficient mechanism is reponsible for the large intensity gain. Apart from the inherent errors of the used theoretical approach, some of the discussed effects might be induced by the solvent, which was not taken into consideration. Overall, both the calculated vertical band centers and the trends in oscillator strengths visible on folding the molecule indicate that the appearance of the spectrum in nonpolar solvents[16,35] is more consistent with a folded equilibrium geometry assumed by DD in the solution.

C. n$-\pi^*$ transitions. As expected, the replacement of the out-of-plane by the in-plane oxygen lone pairs in the active space has only a minimal effect on the ground state (1^1A_g) geometric parameters (Table 1) and the CASSCF energy, whereas the effect on the CASPT2 energy is somewhat larger (~0.002 hartree). The CASSCF references of the n-π^* excited states are dominanted by the shifts of the electron density from the $12a_g$ orbital to the π-orbital of the appropriate symmetry, whereas the excitations from the $10b_{1u}$ remain of minor importance.

Within the second-order approach, the n-π^* excited states, with the exception of ^1A_u and ^3A_u, exhibit problems with the intruder states. A detailed discussion on the emergence and resolving of the intruder states, as well as graphs showing the dependence of the CASPT2 n-π^* excitation energies upon the applied values of the real (ϵ) and imaginary (σ) level shift parameters, are available as Supporting Information. The recommended values of the ϵ and σ parameters are the smallest ones, which stabilize the excitation energies, in the sense that the problems due to the intruder states are solved. Thus upon increasing the parameter further from the recommended value, only a mild change in the excitation energies, normally an increase, is expected. The final, tabulated set of energies (Table 3) is the one obtained using the recommended value of the σ parameter of 0.20 hartree.

Unlike the situation with the $\pi-\pi^*$ transitions, the calculated n-π^* excitation energies place the corresponding bands in the vacuum ultraviolet region of the electronic spectrum (>6.2 eV). With the exception of $^1B_{2g}$ and $^3B_{2g}$, the n-π^* states should occur below the first ionization threshold of DD (7.598 ± 0.002 eV).[17] Within the D_{2h} symmetry, the only dipole allowed n-π^* transition, albeit with an almost negligible intensity (Table 4), is the *x*-polarized $1B_{3u} \leftarrow 1A_g$ occurring ~0.6 eV below the ionization threshold. A relaxation to the butterfly C_{2v} symmetry is expected to enhance this absorption, possibly significantly, owing to a larger overlap of the p_z oxygen lone pairs with the π-orbitals of the benzene rings. The 1^1B_{1g} state is completely analogous to the $2A_g$ state in that it is vibronic allowed via coupling with the butterfly mode, i.e., dipole allowed in the butterfly C_{2v} symmetry, where it would match the third lowest B_2 state. However, because the corresponding transition is *y*-polarized, it is expected to experience a much larger intensity gain than the $2A_g \leftarrow 1A_g$ transition.

Conclusions

The properties of the singlet and triplet $\pi-\pi^*$ and n-π^* valence excited states of dibenzo-*p*-dioxin (DD) were investigated via the CASSCF/CASPT2 approach[22] with the g_2 modification of the zeroth-order Hamiltonian.[25] The use of the relatively small cc-pVDZ basis set was imposed by the size of the system, as well as the large active spaces employed, which comprised the full π-orbital space. Resorting to the real[27] and imaginary[28] level shift techniques proved necessary in calculating the n-π^* excitation energies to eliminate the singularities due to intruder states.

The calculated excitation energies for the $1^1B_{2u} \leftarrow 1^1A_g$ and $1^3B_{3g} \leftarrow 1^1A_g$ transitions, the two most extensively studied by the experiment,[8,9] are in a very good agreement with the measured data. The CASSCF harmonic vibrational wavenumbers of the ground state exhibit a good correlation with the wavenumbers derived from the IR, Raman, and phosphorescence spectra.[9]

The geometry optimizations of all the excited states end up in a planar D_{2h} minimum. Thus no evidence was found for a C_{2v} butterfly-like relaxation, although the wavenumbers pertaining to the b_{3u} butterfly flapping mode proved exceedingly low in both the ground and the lowest dipole allowed excited state (1^1B_{2u}). The remarkably flat potential for the butterfly motion was verified by the calculations on the folded DD geometries.

According to the CASSCF oscillator strengths, the $2^1B_{2u} \leftarrow 1^1A_g$ and $2^1B_{1u} \leftarrow 1^1A_g$ transitions are by far the most intense, whereas the only allowed n-π^* transition ($^1B_{3u}$) should possess only a modest intensity. The vibronic allowed $2^1A_g \leftarrow 1^1A_g$ transition gains only a small intensity on the butterfly-like folding of the DD molecule. Studies into dependence of the oscillator strengths on the extent of the folding show that the experimental electronic spectrum in solution[35] is more consistent with a butterfly-folded equilibrium geometry of DD. An excellent reproduction of the electronic spectrum can be obtained provided minor adjustments are made to the vertical band centers calculated in a mildly folded geometry. At the same time, however, the $2^1A_g \leftarrow 1^1A_g$ oscillator strength has to be increased considerably (75 times), to reproduce faithfully the shape of the 265−310 nm region. This large discrepancy remains unresolved, knowing that the remaining oscillator strengths exhibit a very good agreement with those derived from the experimental spectrum.

Acknowledgment. This work was supported by the Ministry of Science and Technology of the Republic of Croatia under project number 0098033.

Supporting Information Available: A detailed discussion on the intruder states emerging in the CASPT2 calculations on the π^* transitions, graphs depicting dependence of the CASPT2 excitation energy upon various values of real and imaginary level shifts, pictorial representation of the (16,14) active space, and corresponding active occupancies. This material is available free of charge via the Internet at http://pubs.acs.org.

References and Notes

(1) (a) *Sax's Dangerous Properties of Industrial Materials*, 10th ed.; Lewis, R. J., Sr., Ed.; John Wiley & Sons: 2000; Vols. 1−3. (b) Shepard, B. M.; Young, A. L. In *Human and Environmental Risks of Chlorinated Dioxins and Related Compounds*; Tucker, R. E., Young, A. L., Gray, A. P., Eds.; Plenum Press: New York, 1983. (c) Kociba, R. J.; Cabey, O. *Chemosphere* **1985**, *14*, 649. (d) Aylward, L. L.; Hays, S. M.; Karch, N. J.; Paustenbach, D. J. *Environ. Sci. Technol.* **1996**, *30*, 3534. (e) Grassman, J. A.; Masten, S. A.; Walker, N. J.; Lucier, G. W. *Environ Health Perspect.* **1998**, *106*, 761. (f) Hassoun, E. A.; Stohs, S. J. *Comp. Biochem. Physiol.* **1996**, *113C*, 393. (g) Mackie, D.; Liu, J.; Loh, Y.-S.; Thomas, V. *Environ. Health Perspect.* **2003**, *111*, 1145. (h) Williamson, M. A.; Gasiewicz, T. A.; Opanashuk, L. A. *Toxicol. Sci.* **2005**, *83*, 340.

(2) Rappe, C.; Öberg, L. G.; Andersson, R. *Organohalogen Compd.* **1999**, *43*, 249.

(3) Rappe, C. *Pure Appl. Chem.* **1996**, *68*, 1781.

(4) Yoneda, K.; Ikeguchi, T.; Yagi, Y.; Tamade, Y.; Omori, K. *Chemosphere* **2002**, *46*, 1309.

(5) (a) Atkinson, R. Atmospheric chemistry of PCBs, PCDDs, and PCDFs. In *Chlorinated Organic Micropollutants: Issues in Environmental Science and Technology*; Hester, R. E., Harrison, R. M., Eds.; The Royal Society of Chemistry: Cambridge, U.K., 1996. (b) Baker, J. I.; Hites, R. A. *Environ. Sci. Technol.* **2000**, *34*, 2879.

(6) (a) Shiu, W. Y.; Doucette, W.; Gobas, F. A. P. C.; Andren, A.; Mackay, D. *Environ. Sci. Technol.* **1988**, *22*, 651. (b) Sabljić, A. *Chemosphere* **2001**, *43*, 363. (c) Fuster, G.; Schumacher, M.; Domingo, J. L. *Environ. Sci. Pollut. R.* **2002**, *9*, 241. (d) Ogura, I. *Organohalogen Compd.* **2004**, *66*, 3376.

(7) (a) Khasawneh, I. M.; Winefordner, J. D. *Talanta* **1988**, *35*, 267. (b) Funk, D. J.; Oldenborg, R. C.; Dayton, D.-P.; Lacosse, J. P.; Draves, J. A.; Logan, T. J. *Appl. Spectrosc.* **1995**, *49*, 105. (c) Klimenko, V. G.; Nurmukhametov, R. N. *J. Fluoresc.* **1998**, *8*, 129. (d) Harada, H.; Tanaka, M.; Murakami, M.; Shimizu, S.; Yatsuhashi, T.; Nakashima, N.; Sakabe, S.; Izawa, Y.; Tojo, S.; Majima, T. *J. Phys. Chem. A* **2003**, *107*, 6580.

(8) Baba, M.; Doi, A.; Tatamitani, Y.; Kasahara, S.; Katô, H. *J. Phys. Chem. A.* **2004**, *108*, 1388.

(9) (a) Klimenko, V. G.; Nurmukhametov, R. N.; Gastilovich, E. A. *Opt. Spectrosc.* **1997**, *83*, 84. (b) Gastilovich, E. A.; Klimenko, V. G.; Korol'kova, N. V.; Rauhut, G. *Chem. Phys.* **2001**, *270*, 41. (c) Gastilovich, E. A.; Klimenko, V. G.; Korol'kova, N. V.; Nurmukhametov, R. N. *Chem. Phys.* **2002**, *282*, 265.

(10) (a) Schutte, C. J. H.; Bertie, J. E.; Bunker, P. R.; Hougen, J. T.; Mills, I. M.; Watson, J. K. G.; Winnewisser, B. P. *Pure Appl. Chem.* **1997**, *69*, 1633. (b) Schutte, C. J. H.; Bertie, J. E.; Bunker, P. R.; Hougen, J. T.; Mills, I. M.; Watson, J. K. G.; Winnewisser, B. P. *Pure Appl. Chem.* **1997**, *69*, 1641.

(11) Grainger, J.; Reddy, V. V.; Patterson, D. G., Jr. *Appl. Spectrosc.* **1988**, *42*, 643.

(12) Colonna, F. P.; Distefano, G.; Galasso, V.; Irgolic, K. J.; King, C. E.; Pappalardo, G. C. *J. Organomet. Chem.* **1978**, *146*, 235.
(13) Davies, M.; Swain, J. *Trans. Faraday. Soc.* **1971**, *67*, 1637.
(14) Rauhut, G.; Pulay, P. *J. Am. Chem. Soc.* **1995**, *117*, 4167.
(15) Wratten, R. J.; Ali, M. A. *Mol. Phys.* **1967**, *13*, 233.
(16) Lamotte, B.; Berthier, G. *J. Chim. Phys.* **1966**, *63*, 369.
(17) Zimmermann, R.; Boesl, U.; Lenoir, D.; Kettrup, A.; Grebner, Th. L.; Neusser, H. J. *Int. J. Mass Spectrom. Ion Processes* **1995**, *145*, 97.
(18) (a) Roos, B. O.; Taylor, P. R.; Siegbahn, P. E. M. *Chem. Phys.* **1980**, *48*, 157. (b) Roos, B. O. Multiconfigurational (MC) Self-Consistent Field (SCF) Theory. In *European Summerschool in Quantum Chemistry, Book II*; Roos, B. O., Widmark, P.-O., Eds.; Lund University: Lund, Sweden, 2000; pp 285−360.
(19) Andersson, K.; Malmqvist, P.-Å.; Roos, B. O. *J. Chem. Phys.* **1992**, *96*, 1218.
(20) (a) Ljubić, I.; Sabljić, A. *J. Phys. Chem. A* **2002**, *106*, 4745. (b) Ljubić, I.; Sabljić, A. *Chem. Phys.* **2005**, *309*, 157. (c) Ljubić, I.; Sabljić, A. *J. Phys. Chem. A* **2005**, *109*, 2381.
(21) Ljubić, I.; Sabljić, A. *Chem. Phys. Lett.* **2004**, *385*, 214.
(22) Roos, B. O.; Andersson, K.; Fülscher, M. P.; Serrano-Andrés, L.; Pierloot, K.; Merchán, M.; Molina, V. *J. Mol. Struct. THEOCHEM* **1996**, *388*, 257.
(23) Roos, B. O.; Andersson, K.; Fülscher, M. P.; Malmqvist, P.-Å.; Serrano-Andrés, L.; Pierloot, K.; Merchán, M. Multiconfigurational Perturbation Theory: Applications in Electronic Spectroscopy; In *Advances in Chemical Physics: New Methods in Computational Quantum Mechanics*; Prigogine, I., Rice, S. A., Eds.; John Wiley & Sons: New York, 1996; Vol. XCIII: 219.
(24) (a) Lee, J. E.; Choi, W.; Mhin, B. J.; Balasubramanian, K. *J. Phys. Chem. A* **2004**, *108*, 607. (b) Kim, S.; Kwon, Y.; Lee, J.-P.; Choi, S.-Y.; Choo, J. *J. Mol. Struct.* **2003**, *655*, 451. (c) Hirokawa, S.; Imasaka, T.; Urakami, Y. *J. Mol. Struct. THEOCHEM* **2003**, *622*, 229. (d) Wang, Z. Y.; Zhai Z. C.; Wang L. S.; Chen J. L.; Kikuchi O.; Watanabe T. *J. Mol. Struct. THEOCHEM* **2004**, *672*, 97. (e) Taylor, P. H.; Yamada, T.; Neuforth, A. *Chemosphere* **2005**, *58*, 243. (f) Mizukami, Y. *J. Mol. Struct. THEOCHEM* **2005**, *713*, 15.
(25) Andersson, K. *Theor. Chim. Acta* **1995**, *91*, 31.
(26) Anglada, J. M.; Bofill, J. M. *Chem. Phys. Lett.* **1995**, *243*, 151.
(27) Roos, B. O.; Andersson, K. *Chem. Phys. Lett.* **1995**, *245*, 215.
(28) Forsberg, N.; Malmqvist, P.-Å. *Chem. Phys. Lett.* **1997**, *274*, 196.
(29) Dunning, T. H. *J. Chem. Phys.* **1989**, *90*, 1007.
(30) Fülscher, M. P.; Roos, B. O. *Theor. Chim. Acta* **1994**, *87*, 403.
(31) Karlström, G.; Lindh, R.; Malmqvist, P.-Å.; Roos, B. O.; Ryde, U.; Veryazov, V.; Widmark, P.-O.; Cossi, M.; Schimmelpfennig, B.; Neogrady, P.; Seijo, L. *Comput. Mater. Sci.* **2003**, *28*, 222.
(32) (a) Malmqvist, P.-Å. *Int. J. Quantum Chem.* **1986**, *30*, 479. (b) Malmqvist, P.-Å.; Roos, B. O. *Chem. Phys. Lett.* **1989**, *155*, 189.
(33) Schaftenaar, G.; Noordik, J. H. *J. Comput.-Aided Mol. Des.* **2000**, *14*, 123.
(34) (a) Senma, M.; Taira, Z.; Taga, T.; Osaki, K. *Cryst. Struct. Commun.* **1973**, *2*, 311. (b) Singh, P.; McKinney, J. D. *Acta Crystallogr.* **1978**, *B34*, 2956.
(35) Ryzhikov, M. B.; Rodionov, A. N.; Stepanov, A. N. *Zh. Fiz. Khim.* **1989**, *63*, 2125 (in Russian).
(36) McHale, J. L. *Molecular Spectroscopy*; Prentice Hall: Englewood Cliffs, NJ, 1999; pp 167−170.